Development of a dimensionless model for pesticide spraying in agricultural robotics

Ashish Meshram[1*], Kavita Meshram[2], Anil Vanalkar[3], Girish Mehta[4]

(1. Department of Aeronautical Engineering, Priyadarshini College of Engineering Maharashtra, Nagpur, 440019, India;
2. Department of Computer Science & Engineering, St. Vincent Pallotti college of Engineering & Technology, Maharashtra, Nagpur, 441108, India;
3. Department of Mechanical Engineering, K.D.K. College of Engineering, Maharashtra, Nagpur, 440024, India;
4. Department of Mechanical Engineering, Priyadarshini College of Engineering Maharashtra, Nagpur, 440019, India.)

Abstract: Pesticide application plays a vital role in modern agriculture by protecting crops from pests and diseases, thereby improving yield and food security. However, manual spraying methods continue to expose farmers and agricultural workers to hazardous chemicals, often leading to severe health complications. To address these challenges, this paper presents a systematic approach using the Buckingham Pi theorem to develop a dimensionless model that captures the essential relationships governing pesticide spraying processes. The study focuses on key variables such as pesticide volume and plant scan time two critical factors that influence the efficiency and effectiveness of spraying operations. Through dimensional analysis, a generalized predictive equation is derived, enabling the characterization and optimization of spraying performance under varying operational conditions. The resulting model serves as a foundational tool for enhancing the control logic of robotic spraying systems, ensuring more uniform and targeted pesticide application. This approach minimizes wastage, reduces environmental contamination, and significantly improves operator safety by limiting human exposure. Furthermore, the integration of robotics with mathematical modeling underscores the potential for innovative, data-driven solutions in precision agriculture. The research contributes to the development of intelligent spraying systems that are both environmentally sustainable and economically viable, marking a significant advancement in agricultural automation and safety.

Keywords: pesticide spraying, agricultural robotics, buckingham pi theorem, dimensional analysis, mathematical modeling, sustainable farming

Citation: Meshram A., Meshram K.,Vanalkar A,. and Mehta.G.,2026. Development of a dimensionless model for pesticide spraying in agricultural robotics. Agricultural Engineering International: CIGR Journal, 28(1):247-268.

1 Introduction

Agriculture is fundamental to human survival, providing essential resources such as food, fuel, and bedding while employing a large portion of the global population (Meshram et al., 2024). In India, agriculture is particularly crucial as 70% of rural households depend on farming (Jat et al., 2023; Zhang et al., 2024). However, one of the most hazardous tasks in agriculture is pesticide application. Although essential for protecting crops from pests and diseases (Han et al., 2024). Manual pesticide spraying does not fully safeguard farmworkers from exposure, even when protective gear is used (Lochan et al., 2024). Moreover, improper pesticide use can lead to high residue levels in food and contribute to increased chemical resistance

Received date: 2025-04-15 **Accepted date:** 2025-11-19

***Corresponding author: Ashish Meshram**. Department of Aeronautical Engineering, Priyadarshini College of Engineering Maharashtra, Nagpur, 440019, India. Email:anshanandi512@gmail.com.

(Chouriya et al., 2024). To improve safety and efficiency, the automation of pesticide application is being explored through robotics, integrating mechanical, electrical, and computer-based control systems (Bhute et al., 2023; Kaushik et al., 2022). This approach enhances precision in pesticide use while reducing human involvement and associated risks (Sulaiman et al., 2022). Current pesticide application methods, such as manual and battery-operated sprayers, have significant drawbacks, including labor-intensive operation and potential health risks due to exposure the proposed approach minimizes human exposure to hazardous chemicals during pesticide spraying by integrating robotics system with a developed mathematically modeled control system. By applying the Buckingham Pi theorem, the study develops a dimensionless predictive model that optimizes key parameters such as pesticide volume and plant scan time, ensuring efficient and uniform application. By incorporating this model into the control logic of robotic spraying systems, the need for manual spraying is significantly reduced, thereby limiting direct contact between operators and toxic chemicals. This systematic and data-driven approach not only enhances spraying precision and reduces environmental pollution but also greatly improves operator safety by minimizing exposure to hazardous substances during agricultural operations also reduce the farmer death (Dou et al., 2023; Dhutekar et al., 2021).

In enclosed environments like greenhouses, workers face increased exposure to toxins during spraying, further exacerbating health risks (Trivedi et al., 2021). Additionally, the overuse of pesticides leads to chemical resistance in pests, posing challenges to crop protection (Abade et al., 2021). This paper addresses these challenges by proposing a robotic pesticide spraying system that reduces human exposure and enhances precision in application, thereby overcoming the inefficiencies of manual methods. Specifically, it aims to develop a mathematical model for a robotic pesticide spraying system using dimensional analysis to improve efficiency and safety in agricultural settings. The model focuses on optimizing pesticide application by minimizing human intervention while maintaining precision and control. Pesticide volume and plant scan time are considered critical variables in the study because they directly influence the efficiency, effectiveness, and precision of the pesticide spraying process. The pesticide volume determines the amount of chemical applied to the plant, which affects both the quality of pest control and the potential for chemical wastage or environmental contamination. Applying too much pesticide can harm the environment and increase costs, while too little may lead to ineffective pest control. Similarly, the plant scan time represents the duration or speed at which the robotic system scans and targets plants, affecting how accurately and uniformly the pesticide is applied. An optimal scan time ensures that each plant receives the appropriate amount of pesticide without over spraying or missing areas. Therefore, these two variables are very important for achieving a balance between effective pest control, resource efficiency, and environmental and operator safety in robotic pesticide spraying systems.

Agriculture is a cornerstone of human survival, providing essential resources such as food, fuel, and bedding while employing a significant portion of the global population (Meshram et al., 2024; Jat et al., 2023). In India, agriculture is particularly vital, with 70% of rural households depending on farming as their primary occupation (Bechar and Vigneault, 2016; García-Alegre et al., 2001; Ramesh and Pasupathy, 2019). One of the critical yet hazardous tasks in agriculture is the application of pesticides to crops to protect them from harmful organisms. Farmers strive to produce higher-quality crops and increase yields, but their efforts are frequently hindered by pests, insects, and fungal infections. Manual pesticide application, despite the use of protective measures such as gloves, masks, and aprons, does not fully safeguard farmers and farmworkers from exposure (Bhute et al., 2023; Kaushik et al., 2022). Battery-operated and hand-compressed sprayers are commonly used for pesticide spraying (Kassim et al., 2020; Budiharto et al., 2019; Song et al., 2015; Olabi et al., 2022; Shaw and Vimalkumar, 2020). However, manual methods have several drawbacks, including the physical effort required to transport and

carry the sprayers to the application site. Additionally, the risk of over-spraying increases, which can pose significant health hazards.

In enclosed environments such as greenhouses, these risks are further exacerbated, as workers are exposed to higher concentrations of toxins during spraying (Ozgul and Celik, 2018; Pandey et al., 2020). Furthermore, the overuse of pesticides leads to high residue levels in food and contributes to increased resistance to chemicals, posing additional challenges to sustainable agriculture. conventional chemical control technology (Karunarathne et al., 2020). Thus a proper measure should be taken for more efficient, safer application methods (Prechsl et al., 2022). By automating this process using mobile robots, human contact with pesticide-sprayed fields can be minimized, making pesticide application more precise and efficient. This approach integrates mechanical, electrical, electronic, and computer-based control systems, which are commonly used in product design to meet customer requirements. For example, robotic pesticide spraying involves a mechatronic structure that enhances precision and reduces human exposure to harmful chemicals (Salotti and Suhir, 2024).

The primary objective of this paper is to develop a mathematical model for a mobile robot that efficiently targets and applies pesticides. Corporations are integrating advanced robotics, artificial intelligence, vision technology, and control systems into automation processes to enhance efficiency and precision (Li et al., 2023). While removing human intervention from manual labor tasks with automated solutions developed by a range of academies delivering technical challenges about Industry 4.0 issues engineers might have at hand for solving problems in more detail (Reji and Kumar, 2023; Ray et al., 2023). This paper presents a comprehensive robotic system for pesticide application in an agricultural setting, aimed at improving efficiency, enhancing control for farmers, and increasing their safety. It details the integration of various technologies, including microcontrollers, sensors, actuators, and computer-based control systems, into a robotic pesticide spraying system (Patil, 2023). (Kaushik and Shankar, 2022; Mehta et al., 2019).

Overall, several fascinating studies have demonstrated how the Buckingham Pi theorem can enhance the generalization ability of machine learning models. However, many questions remain about how such techniques might perform in other domains and with experimental data, as most results are based on highly simplified simulated experiments, particularly in the context of pest prediction. In this research, propose a mathematical model using a dimensional analysis approach for a pesticide-spraying robot designed to address pest attacks in agriculture (Gu et al., 2019). As far as only a small number of initiatives have looked into the idea of dimensional analysis in the context of motion control and robotics. (Bucelli et al., 2023)

The authors proposed an improved kinematic calibration technique based on dimensionless error mapping matrices (EMMs) (Luo et al., 2021; Ilyushin and Kapostey, 2023). According to the simulation results, in a variety of units, the residual pose errors with the suggested dimensionless EMMs were less than those with the traditional EMM. Finally, the idea of dimensionless policies is introduced in Girard (2024) Additionally, this study makes a significant contribution by demonstrating that, unlike previous research, which primarily relies on simulated data, the effectiveness of the proposed method was also validated through real-world experiments using miniature autonomous robots under ideal conditions (Normey-Rico et al., 2001; Fue et al., 2020). (Gu. et al. 2019; Prakash et al., 2021). A method based on particular relationships that shouldn't depend on units is made up of dimensionless numbers and dimensional analysis, and it can be used to examine a variety of physical problems (Reyes et al., 2022). The concept of matching ratios, such as Reynolds, Prandt, or Mach numbers, in fluid mechanics enables the generalization of experimental findings across systems with various sizes. The current success of data-driven schemes and machine learning focuses the problem of insights, and dimensional analysis is being applied in the learning context once more (Bakarji et al., 2022; Xie et al., 2022).

The literature highlights significant advancements in agricultural automation, particularly in pesticide spraying robots. The integration of robotics, Artificial Intelligence, and control systems has improved the efficiency and precision of pesticide application while reducing human exposure to harmful chemicals. The Buckingham π theorem and dimensional analysis have proven valuable in simplifying complex interactions and enhancing model generalization, particularly in machine learning and motion control applications. However, challenges remain, particularly regarding the applicability of dimensional analysis across different robotic systems and real-world agricultural settings. Most studies rely on simulated environments, necessitating further validation through field experiments. Future research should focus on refining mathematical models to accommodate varying agricultural conditions, improving the adaptability of dimensionless methods for diverse robotic applications, and integrating machine learning techniques to enhance pest prediction accuracy. Addressing these gaps will ensure more robust, efficient, and practical automated pesticide spraying solutions for sustainable agriculture.

2 Materials and methods

2.1 Experimental approach

The design of experimentation is a structured approach used in the research process to systematically plan, execute, and analyze experiments. It is an essential methodology that enables researchers to examine the relationship between independent variables and dependent (response) variables. This approach helps determine cause-and-effect relationships, streamline procedures, improve quality, and obtain reliable results. The design of experimentation involves careful planning to meet specific research objectives. Proper experimental planning is crucial for achieving research goals efficiently and clearly, ensuring the collection of appropriate data with a suitable sample size.

2.2 Variable identification

Mathematical model represents a physical system through a set of variables and equations that describe the interdependencies among those variables. These models provide a structured framework to analyse system behaviour and predict outcomes under varying conditions. During experimental procedures, data are collected corresponding to both independent and dependent (response) variables, which are critical to model formulation and validation. The term variable broadly refers to any measurable physical quantity that can vary. A quantity that varies independently of others is designated as an independent variable, while a quantity that changes in response to one or more independent variables is classified as a dependent variable. This distinction is essential for understanding the cause-and-effect relationships within the system.

For the pesticide-spraying robotic system under investigation, all relevant physical quantities are identified and categorized into dependent and independent parameters, as summarized in Table 1. Each parameter is subsequently expressed in terms of its fundamental dimensional units using the MLT (Mass-Length-Time) system, along with its associated symbol and physical unit. This dimensional representation facilitates the application of dimensional analysis, including the use of the Buckingham Pi theorem, to derive a dimensionless model that characterizes the essential dynamics of the spraying process.

2.3 Dimensional analysis

Dimensional analysis is carried out to establish dimensionless equations in terms of various independent and dependent dimensionless groups of physical quantities affecting the system.

2.3.1 Derivation of π terms from dependent and independent variables'

The Buckingham Pi theorem is employed to formulate a dimensionless model of the system by applying principles of dimensional analysis. This method facilitates the reduction of complex physical relationships into a simplified set of dimensionless groups, thereby enabling generalized and scalable modeling. As summarized in Table 2, a total of 18 physical variables have been identified, including both independent and dependent parameters relevant to the pesticide-

spraying robotic system. Among these, 15 variables are classified as independent, and 3 are selected as repeating variables for constructing the π terms. According to the Buckingham Pi theorem, the number of resulting dimensionless π terms is given by:

$$\text{Number of } \pi \text{ terms} = n - m = 15 - 3 = 12$$

Where,

n = total number of independent variables = 15;

m = number of repeating variables = 3.

Table 1 Categorization of independent and dependent variables

Sr. No.	Variables	(Dependent/Independent)	Symbols	Unit	Dimensions
01	Height of robot	Independent	H	m	$M^0L^1T^0$
02	Width of robot	Independent	B	m	$M^0L^1T^0$
03	Weight of robot	Independent	M	kg	$M^1L^0T^0$
04	Acceleration due to gravity	Independent	G	m s^{-2}	$M^0L^1T^{-2}$
05	Height of robot base	Independent	H_r	m	$M^0L^1T^0$
06	Wheel diameter	Independent	D	m	$M^0L^1T^0$
07	Robot speed	Independent	N	m s^{-1}	$M^0L^1T^{-1}$
08	Height of plant	Independent	H_p	m	$M^0L^1T^0$
09	Distance between two Plant	Independent	L	m	$M^0L^1T^0$
10	pesticide remaining in tank	Independent	V_t	m^3	$M^0L^3T^0$
11	Height of link	Independent	L_l	m	$M^0L^1T^0$
12	Link rotational speed	Independent	W	m s^{-1}	$M^0L^1T^{-1}$
13	Pest detection accuracy	Independent	A	Dimension less	$M^0L^0T^0$
14	Pesticide viscosity	Independent	μ	N-s m^{-3}	$M^1L^{-1}T^{-1}$
15	Pesticide spraying force	Independent	F	N	$M^1L^1T^{-2}$
16	Pesticide volume	Dependent	V_s	m^3	$M^0L^3T^0$
17	Plant scan time	Dependent	T	sec	$M^0L^0T^1$
18	No. of pest detected	Dependent	N	Dimension less	$M^0L^0T^0$

The resulting 12 dimensionless groups (π terms) capture the core functional relationships among the system variables and form the foundation for developing the predictive model. These groups are essential for understanding the influence of key parameters on the system's response and for optimizing the pesticide-spraying process in a generalized, scalable, and technology-agnostic manner. The repeating variables H, g, and μ were selected in the Buckingham Pi analysis based on their dimensional independence, physical relevance, and ability to represent the fundamental dimensions of the system mass (M), length (L), and time (T). Specifically, H (height or characteristic length) captures the geometric aspect of the spraying setup, g (gravitational acceleration) accounts for the external force acting on the system, and μ (fluid viscosity) represents the internal fluid property influencing spray flow and droplet formation. These variables collectively provide a comprehensive representation of geometry, external physical influence, and fluid behavior. While alternative sets of repeating variables could be used if they meet the same dimensional and physical criteria, such choices would only change the form of the resulting π terms, not the underlying physical relationships or the predictive capability of the final model.

2.3.2 The selection of repeating variables for the dimensionless approach

In dimensional analysis, the repeating variables are

typically selected based on precise criteria to ensure that they capture the fundamental aspects of the system and can form dimensionless groups with other variables. Table 2 list of repeating variables used in your analysis. These are fundamental variables that appear repeatedly in the dimensional analysis of system.

Table 2 Identification of repeating variables in Buckingham Pi theorem application

Sr. No.	Description of Variables	Types of Variables	Symbols	Unit	Dimensions
01	Height of Robot	Independent	H	m	$M^0L^1T^0$
02	Acceleration due to gravity	Independent	G	m s^{-2}	$M^0L^1T^{-2}$
03	Pesticide viscosity	Independent	μ	Pa sec	$M^1L^{-1}T^{-1}$

2.3.3 Formation of Pi-Terms for independent variables

The application of Buckingham Pi theorem in this study utilizes fundamental physical quantities to express all independent and dependent variables in terms of the MLT (Mass-Length-Time) system. Specifically, M represents Mass, with its unit in kilograms (kg); L denotes Length, measured in meters (m); and T corresponds to Time, with its unit in seconds (s). All variables in the system both independent and dependent—are expressed using these base dimensions. The resulting equations, as derived through the dimensional analysis process, adhere to this principle and are formulated accordingly.

(1) First π term

$$\pi_1 = (H)^a(g)^b(\mu)^cB \quad (1)$$

Substitution of Dimensional Quantities into the Equation:

$M^0L^0T^0 = [\ M^0L^1T^0\ ]^a\ [M^0L^1T^{-2}]^b\ [M^1L^{-1}\ T^{-1}]^c\ [M^0L^1T^0]$

Equating the dimensions on both sides.

mass: 0=c, a=-1; length: 0=a+b−c+1, b=0; time0=2b−c, c = 0.

Substituting the values a, b, c in the equation of π1 term.

$$\pi\ 1 = (H)a(g)b(\mu)cB$$

Therefore, the final equation is:

$$\pi_1 = \left[\frac{B}{H}\right]$$

(2) Second π term

$$\pi\ 2 = (H)a(g)b(\mu)cM \quad (2)$$

Substitution of Dimensional Quantities into the Equation.

$M^0L^0T^0=[M^0L^1T^0]^a[M^0L^1T^{-2}]^b[M^1L^{-1}T^{-1}]^cM^1L^0T^0]$

Equating the dimensions on both sides, Substituting the values a, b, c in the equation of π2 term in equation $\pi_2 = (H)^a(g)^b(\mu)^cM$.

Therefore, the final equation is:

$$\pi_2 = \left[\sqrt{\frac{g}{H^3}}\frac{M}{\mu}\right]$$

(3) Third π term

$$\pi_3 = (H)^a(g)^b(\mu)^cHr \quad (3)$$

Substitution of Dimensional Quantities into the Equation.

$M^0L^0T^0=[M^0L^1T^0]^a[M^0L^1T^{-2}]^b[M^1L^{-1}T^{-1}]^cM^0L^1T^0]$

Equating the dimensions on both sides.

Therefore, the final equation is of $\pi_3 = (H)^a(g)^b(\mu)^{cH}$.

mass: 0=c, a=-1; length 0=a+b−c+1,b = 0; Time 0−2b−c, c = 0.

$$\pi_3 = \left[\frac{H_r}{H}\right]$$

(4) Fourth π term

$$\pi_4 = (H)^a(g)^b(\mu)^cD \quad (4)$$

Substitution of Dimensional Quantities into the Equation.

$M^0L^0T^0=[M^0L^1T^0\ ]^a[M^0L^1T^{-2}]^b[M^1L^{-1}\ T^{-1}]^c\ [M^0L^1T^0]$

Equating the dimensions on both sidest:

mass: 0=c, a=-1; length: 0=a+b−c+1,b = 0; time: 0−2b−c, c = 0.

Therefore, the final equation of $\pi_4 = (H)^a(g)^b(\mu)^cD$

$$\pi_4 = \left[\frac{D}{H}\right]$$

(5) Fifth π term

$$\pi_5 = (H)^a(g)^b(\mu)^cN \quad (5)$$

Substitution of Dimensional Quantities into the Equation.

$M^0L^0T^0=[M^0L^1T^0]^a[M^0L^1T^{-2}]^b[M^1L^{-1}T^{-1}]^c\ [M^0L^1T^{-1}]$

mass: 0=c, a=-1/2, b=-1/2, c=0; length: 0=a+b−c+1,b = -1/2; time: 0 = 0−2b−c-1, c = 0.

Therefore, the final equation is $\pi_5 = (H)^a(g)^b(\mu)^cN$

$$\pi_5 = \left[\frac{N}{\sqrt{Hg}}\right]$$

(6) Sixth π term

$$\pi_6 = (H)^a(g)^b(\mu)^c H_p \quad (6)$$

Substitution of Dimensional Quantities into the Equation

$M^0L^0T^0 = [\ M^0L^1T^0\ ]^a[M^0L^1T^{-2}]^b[M^1L^{-1}\ T^{-1}]^c [M^0L^1T^0]$

Equating the dimensions on both sides.

Mass 0=c, a=-1;Length:0=a+b−c+1,b = 0;Time 0−2b−c,c = 0.

Therefore, the final equation is $\pi_6 = (H)^a(g)^b(\mu)^c H_p$

$$\pi_6 = \left[\frac{H_p}{H}\right]$$

(7) Seventh π term

$$\pi_7 = (H)^a(g)^b(\mu)^c L \quad (7)$$

Substitution of Dimensional Quantities into the Equation

$M^0L^0T^0=[M^0L^1T^0]^a[M^0L^1T^{-2}]^b[M^1L^{-1}T^{-1}]^c[M^0L^1T^0]$

mass: 0=c, a=-1, b = 0,c = 0 ; length: 0=a+b−c+1 b = 0; time: 0−2b−c, c = 0.

Equating the dimensions on both sides of $\pi_7 = (H)^a(g)^b(\mu)^c L$

Therefore, the final equation is:

$$\pi_7 = \left[\frac{L}{H}\right]$$

(8) Eighth π term

$$\pi_8 = (H)^a(g)^b(\mu)^c Vt \quad (8)$$

Substitution of Dimensional Quantities into the Equation

$M^0L^0T^0=[M^0L^1T^0]^a[M^0L^1T^{-2}]^b[M^1L^{-1}T^{-1}]^cM^0L^3T^0]$

Equating the dimensions on both sides.

mass: 0=c, a=-3, b = 0 c = 0; length: 0=a+b−c+3, b = 0; time: 0−2b−c, c = 0.

Therefore, the final equation is $\pi_8 = (H)^a(g)^b(\mu)^c Vt$

$$\pi_8 = \left[\frac{Vt}{H^3}\right]$$

(9) Nine π term

$$\pi_9 = (H)^a(g)^b(\mu)^c L_1 \quad (9)$$

Substitution of Dimensional Quantities into the Equation

$M^0L^0T^0=[M^0L^1T^0]^a[M^0L^1T^{-2}]^b[M^1L^{-1}T^{-1}]^c[M^0L^1T^0]$

mass: 0=c, a=-1, b = 0, c = 0 ; length: 0=a+b−c+1,b = 0 ; time: 0−2b−c, c = 0.

Therefore, the final equation is $\pi_9 = (H)^a(g)^b(\mu)^c L_1$.

$$\pi_9 = \left[\frac{L_1}{H}\right]$$

(10) Tenth π term

$$\pi_{10} = (H)^a(g)^b(\mu)^c w \quad (10)$$

Substitution of Dimensional Quantities into the Equation

$M^0L^0T^0=[M^0L^1T^0]^a[M^0L^1T^{-2}]^b[M^1L^{-1}T^{-1}]^c\ [M^0L^1T^{-1}]$

mass: 0=c, a=-1/2 ; length: 0=a+b−c+1, b = -1/2 ; time: 0 = 0-2b-c-1,c = 0.

Therefore, the final equation is $\pi_{10} = (H)^a(g)^b(\mu)^c w$.

$$\pi_{10} = \left[\frac{w}{\sqrt{Hg}}\right]$$

(11) Eleventh π term

$$\pi_{11} = (H)^a(g)^b(\mu)^c \alpha \quad (11)$$

Substitution of Dimensional Quantities into the Equation.

$M^0L^0T^0 = [M^0L^1T^0]^a\ [M^0L^1T^{-2}]^b[M^1L^{-1}\ T^{-1}]^c [M^0L^0T^0]$

mass: 0=c,a= 0, b = 0, c = 0 ; length: : 0=a+ b−c,b = 0 ; time: 0 = 0−2b−c, c = 0.

Therefore, the final equation is $\boldsymbol{\pi}_{11} = (H)^a(g)^b(\mu)^c\alpha$.

$$\pi_{11} = [\alpha]$$

(12) Twelfth π term

$$\pi_{12} = (H)^a(g)^b(\mu)^c F \quad (12)$$

Substitution of Dimensional Quantities into the Equation.

$M^0L^0T^0 = [\ M^0L^1T^0\ ]^a[M^0L^1T^{-2}]^b[M^1L^{-1}\ T^{-1}]^c [M^1L^1T^{-2}]$

mass: 0=c + 1, a= -3/2 ; length: 0=a+b−c+1,b = -1/2 ;time: 0 = 0−2b−c-2,c = -1.

Therefore, the final equation is $\pi_{12} = (H)^a(g)^b(\mu)^c F$.

$$\pi_{12} = \left[\frac{F}{\sqrt{H^3 g\mu}}\right]$$

The dimensionless π (Pi) terms derived using Buckingham Pi Theorem for dimensional analysis. These π terms facilitate the simplification of complex physical relationships by transforming them into non-dimensional groups, thereby enabling a more general-

ized and scalable representation of the system's behavior. The use of these dimensionless groups allows for the identification of key factors influencing the system and enhances the ability to model, analyze, and optimize its performance under varying conditions as shown in Table 3.

Table 3 Formulation of independent π terms

pi (π) terms	pi (π) terms equation	pi (π) terms	pi (π) terms equation
π_1	$\pi_1 = \left[\frac{B}{H}\right]$	π_7	$\pi_7 = \left[\frac{L}{H}\right]$
π_2	$\pi_2 = \left[\sqrt{\frac{g}{H^3}}\frac{M}{\mu}\right]$	π_8	$\pi_8 = \left[\frac{Vt}{H^3}\right]$
π_3	$\pi_3 = \left[\frac{H_r}{H}\right]$	π_9	$\pi_9 = \left[\frac{L_1}{H}\right]$
π_4	$\pi_4 = \left[\frac{D}{H}\right]$	π_{10}	$\pi_{10} = \left[\frac{w}{\sqrt{Hg}}\right]$
π_5	$\pi_5 = \left[\frac{N}{\sqrt{Hg}}\right]$	π_{11}	$\pi_{11} = [\alpha]$
π_6	$\pi_6 = \left[\frac{H_p}{H}\right]$	π_{12}	$\pi_{12} = \left[\frac{F}{\sqrt{H^3 g\mu}}\right]$

2.3.4 Formation of pi (π) terms for dependent variables

(1) First π_d term

$$\pi_{d1} = (H)^a(g)^b(\mu)^c\ Vs \quad (13)$$

Substituting the dimensions into the equation, we get:

$M^0L^0T^0 = [M^0L^1T^0]^a[M^0L^1T^{-2}]^b[M^1L^{-1}T^{-1}]^c[M^0L^3T^0]$

Equating the dimensions on both sides.

mass: 0=c, a=-3, b = 0 and c = 0; length: 0=a+b−c+3,b = 0; time: 0−2b−c, c = 0

Therefore, the final equation is $\boldsymbol{\pi}_{d1} = (H)^a(g)^b(\mu)^c$ Vs.

$$\pi_{d1} = \left[\frac{Vs}{H^3}\right]$$

(2) Second π_d term

$$\pi_{d2} = (H)^a(g)^b(\mu)^c\ t \quad (14)$$

Substituting the dimensions into the equation.

$M^0L^0T^0 = [M^0L^1T^0]^a[M^0L^1T^{-2}]^b[M^1L^{-1}T^{-1}]^c[M^0L^0T^1]$

Equating the dimensions on both sides.

mass: 0=c, a=-1/2; length: 0=a+b−c, b = ½; time: 0 = 0−2b−c+1 c = 0

Therefore, the final equation is $\boldsymbol{\pi}_{d2} = (H)^a(g)^b(\mu)^c$ t.

$$\pi_{d2} = \left[\sqrt{\frac{g}{H}}t\right]$$

The dimensionless π (Pi) terms corresponding to the dependent variables in the robotic pesticide spraying system. These terms are derived through Buckingham Pi Theorem and represent the relationships between the dependent variables in a non-dimensional form. By converting the physical quantities into dimensionless groups, this approach facilitates the simplification of complex relationships, enabling more efficient analysis and reducing the need for extensive experimental setups. The use of these dimensionless terms enhances the clarity of system behavior, allowing for more generalized and scalable modeling as in the Table 4.

Table 4 Formulation of dependent Pi (π) terms

Pi (π) terms	Pi (π) terms equation
π_{d1}	$\left[\frac{Vs}{H^3}\right]$
π_{d2}	$\left[\sqrt{\frac{g}{H}}t\right]$

2.4 Reduction of variables using dimensional analysis

The variables involved in this process are combined into dimensionless Pi (π) terms, which are formulated based on the respective dimensional identities of the grouped variables. According to Buckingham π Theorem, a physical phenomenon comprises multiple variables, both independent and dependent, each expressed in terms of fundamental dimensions such as mass (M), length (L), and time (T). These variables are then represented as π-terms. The theorem simplifies the problem by reducing its complexity and expressing the relationships between variables as dimensionless

π-terms, thus facilitating easier analysis and interpretation. To further enhance the simplicity and minimize the complexity of the process, the independent π-terms derived above have been refined using the variable reduction method proposed by Schenk Jr. This method allows for a more efficient grouping of the existing π-terms, yielding a new independent π-term by considering the inherent nature of the variables. As a result, four distinct π-terms are formed, which are as follows:

1. The first π term, π_1, is associated with the geometry of the robot, capturing the spatial and structural factors influencing its movement and efficiency.

2. The second πterm, π_2, pertains to the plant, representing the physical characteristics and behaviour of the plant being sprayed.

3. The third π term, π_3, is related to the sensor, incorporating the effects of sensor technology on data acquisition and system performance.

4. The fourth π term, π_4, is linked to the volume, reflecting the impact of pesticide volume on spray distribution and coverage.

As a result, the total 12 π terms corresponding to the independent variables in the pesticide-spraying system have been condensed and organized into these four new π terms, as summarized in Table 5 below the dimensionless Pi (π) terms, which are formulated using the Buckingham π theorem to describe key relationships in a robotic pesticide spraying system. These terms help in reducing the complexity of the system by expressing relationships between variables in a non-dimensional form, which is useful for scaling, optimization, and experimental validation. Additional variables that could be included in the dimensionless model to further enhance spraying performance are those that influence droplet behaviour, coverage uniformity, and energy efficiency during spraying. For instance, diameter of nozzle and spray pressure could be incorporated to account for variations in pesticide droplet size and spray pattern, which directly affect deposition efficiency. Air velocity could be included to represent the impact of environmental conditions on droplet drift and dispersion. Similarly, robot velocity and nozzle-to-target distance are important operational parameters that influence the precision and uniformity of pesticide delivery. Other relevant factors such as fluid density, surface tension, and ambient humidity or temperature could also be considered, as they affect evaporation rate and droplet adhesion on plant surfaces. Including these variables in the dimensionless model would enable a more comprehensive characterization of the spraying dynamics, leading to improved control accuracy, reduced chemical wastage, and optimized performance of the robotic spraying system.

Table 5 π terms in reduced form for independent variables

Pi (Π) terms	Equations	Description
π_1	$\left[\frac{\pi_1}{\pi_4}\right]\left[\frac{\pi_2}{\pi_9}\right]\left[\frac{\pi_3}{\pi_{10}}\right]\left[\frac{\pi_5}{\pi_{12}}\right] = \frac{BH_TMN}{DL_1\omega F}$	π term related to the geometry of the robot
π_2	$\left[\frac{H_p}{H}\right]\left[\frac{L}{H}\right] = \frac{H_pL}{H^2}$	π term related to the plant.
π_3	$[\alpha]$	π term related to the camera and sensor.
π_4	$\left[\frac{Vt}{H^3}\right]$	π term related to the pesticide volume.

2.4.1 Determination of sample size for experimental validation

Selecting an appropriate sample size is a critical component of designing a statistically valid experimental study. Accurate estimation of the required sample size is essential to achieve a desired level of confidence in the results. If the sample size is arbitrarily assumed, the analyst must subsequently determine the confidence limits that correspond to the specified confidence level. Sampling, in this context, involves determining the optimal number of observations necessary to ensure statistical reliability without unnecessary resource expenditure. As a general principle, the sample should be of optimum size large enough to yield precise estimates, yet not excessively large to avoid waste of time and resources.

When the population variance (σ^2) is known, the required sample size n for a confidence level of (α), with a margin of error ±d on either side of the mean, is calculated using the following formula:

$$n = \left[\frac{(Z\alpha/2)(\sigma)}{d}\right]^2$$

Considering the 95% confidence level, from the normal table for 95% probability we have $Z\alpha/2$ =1.96 and α = 0.05. Assuming the estimate should lie within the interval n = μ $\pm$(σ/5) with probability of 0.95 where μ is the population mean.

$$n = \left[\frac{(1.96)(\sigma)}{\sigma/5}\right]^2$$

$$n = 96.04 \approx 96$$

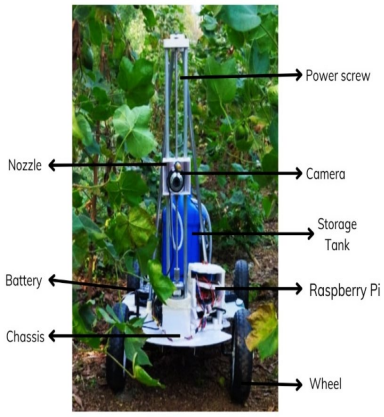

Figure 1 Fabrication and assembly of the pesticide spraying robot

2.4.2 Experimental setup and system configuration

The experimental setup of the pesticide spraying robot was systematically designed and fabricated to facilitate field experimentation in accordance with the predefined experimental plan, as illustrated in Figure 1. The Figure 1 depicts a mobile robotic platform specifically developed for pesticide application in agricultural environments. The robot is engineered to autonomously navigate through crop fields, utilizing sensor-based perception for plant detection, and to perform targeted and efficient pesticide spraying operations. This autonomous functionality enables precise pesticide delivery, minimizing wastage and enhancing coverage uniformity across the treatment area.

The power screw is a mechanical component that facilitates vertical movement, likely adjusting the height of the spraying nozzle for better pesticide application. It ensures that the spray reaches plants of varying heights. The nozzle is responsible for spraying pesticides onto crops. It disperses the liquid in a controlled manner to ensure uniform coverage and minimize Wastage. The camera is used for It assists in identifying infected plants and determining where pesticide application is needed. This tank holds the pesticide solution before it is sprayed onto the crops. It ensures a during operation. The Raspberry Pi is the main computing unit controlling the robot's operation. It processes data from sensors and cameras, enabling autonomous decision-making for navigation and spraying. The battery powers the robotic system, providing energy for motors, sensors, and electronic components. A rechargeable power source allows continuous operation in the field. The chassis is the robot, supporting all the components. It provides stability and protection to the internal systems. The wheels enable mobility, allowing the robot to move through the field. They are designed for rough agricultural terrain, ensuring smooth navigation.

2.4.3 Experimental observations and data recording

A field experiment was conducted in a cotton crop field to evaluate the performance of a pesticide-spraying robot in terms of pest detection accuracy and pesticide application efficiency. The experiment was carried out in an agricultural field located in the Nagpur district, Maharashtra, India. Cotton is typically cultivated in this region during the rainy season, which begins in June. Therefore, the experimental period was selected from August 2023 to March 2024 to capture the critical growth phases of the cotton plants. The total field area selected for the experiment was approximately 4,046.890 square meters, containing 130 cotton plants. These plants were arranged in 13 rows, with 10 plants in each row. Prior to the commencement of the experiment, the pesticide-spraying robot was calibrated to ensure proper functioning of the pest detection and pesticide application systems. This process involved adjusting the sensor systems for accurate plant detection and configuring the convolution neural net-

work based pest detection algorithm to correctly identify pests on the plants.

Additionally, the accuracy of the spraying system specifically droplet size and spray coverage was verified. The navigation system was also tested to ensure smooth and consistent movement along the cotton plant rows. At the beginning of each trial, the robot was positioned at the starting point of the field. Upon receiving an input signal, the wheel motors were actuated, and the robot began traversing the field. During its movement, the robot identified the location of each plant and stopped in front of it. Subsequently, the motor of the power screw mechanism was actuated, causing the moving platform housing the camera and nozzle to elevate and scan the plant in a frame-wise manner. During the vertical scanning motion, the on-board camera captured sequential image frames of the plant and transmitted them to the convolution neural network based pest detection algorithm. This algorithm processed each frame to identify the presence of pests on the plant leaves. Upon detection, a control signal was generated and sent to the spray management system.

In response to this signal, the pesticide pump was actuated, drawing the required volume of pesticide from the storage tank and delivering it through the pipeline to the spray nozzle. The system was programmed to dispense a precise volume of 10 millilitres of pesticide directly onto the detected pest location, ensuring targeted application and minimizing chemical waste.

3 Results

3.1 Model formulation using response surface methodology

Response Surface Methodology (RSM) is a statistical technique useful for developing, improving, and optimizing processes. It is particularly valuable in modelling and analysing problems where multiple variables influence a response variable or output, with the goal of optimizing this response. In the context of a pesticide-spraying robot, RSM can be used to model the relationship between key independent variables (factors) and the output (response), such as the effectiveness of pesticide application, spray uniformity, or pesticide usage efficiency. The primary objective is to determine the optimal conditions for pesticide application to achieve maximum effectiveness with minimal waste. This method involves conducting a series of designed experiments to evaluate the effects of input variables and their interactions on the response. By fitting a polynomial model to the experimental data, RSM helps in understanding complex relationships between variables, identifying optimal conditions, and improving processes across various fields.

The equation for RSM is $y = f(X1, X2) + \varepsilon$

Where, *X1*, and *X2* are process parameters and ε represents the error observed in the response y, if we denote the expected responses by

$$E(y) = f(xX1, xX2) = \acute{\eta}$$

The experiments were designed and conducted using RSM. The response surface model was developed using the statistical software MATLAB. The best-fit regression equations for the selected model were obtained for the response characteristics. The reliability of the first model for pesticide spread (πd_1) in the RSM analysis, despite its low R2 value (0.108) and negative adjusted R2, can be justified by recognizing its preliminary or exploratory role in the modeling process. A low R2 indicates that the selected variables in this initial model explain only a small portion of the variation in pesticide spread, suggesting that key influencing acors might be missing or their interactions are nonlinear. However, such early-stage models are valuable for identifying trends, testing assumptions, and guiding the refinement of experimental design. The negative adjusted R2 highlights that the model may not yet provide a strong predictive fit, but it still offers insight into variable sensitivity and potential directions for improvement in subsequent iterations. In the context of dimensional analysis and RSM, this preliminary model serves as a baseline reference, from which more comprehensive models—incorporating additional parameters or interaction terms can be developed to achieve

higher accuracy and predictive capability. Thus, while the statistical reliability of this specific model is limited, its analytical value lies in informing the optimization and refinement process of the overall system model.

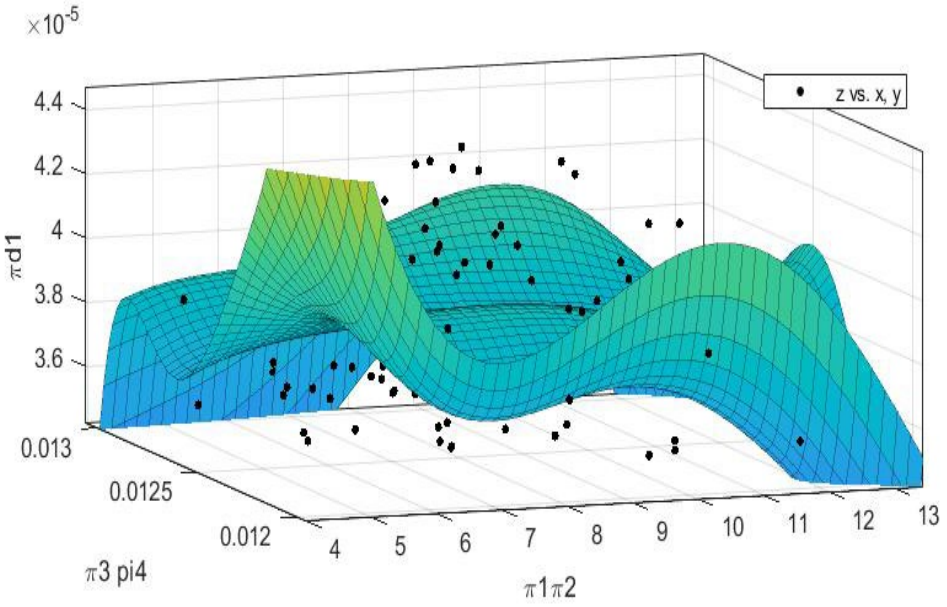

Figure 2 Graphical representation of response surface model for pesticide spread

3.2 Development of response surface model for pesticide quantity spread

Below is a breakdown of each axis and component represents:

Vertical axis (πd1): This represents the plant scan time, which indicates the time required for the robot to scan or cover a particular area in the field.

Horizontal axes:

The axis labelled π1π2 represents the combined effect of the robot's geometry (π1) and another independent variable, possibly related to the robot or spraying process.

The axis labelled π3π4 represents the combined effect of pesticide volume parameters, potentially including factors such as spray volume or nozzle flow rate.

Surface representation: The surface represents a fitted model or mathematical surface, showing how plant scan time (πd1) changes as the values of π1π2 and π3π4 vary.

Surface shape: The shape of the surface indicates non-linear relationships between these variables. Peaks and valleys suggest points where the plant scan time significantly increases or decreases based on different combinations of π1π2 and π3π4.

Figure 2 shows the relationship between several variables in the pesticide-spraying robot.

Black dots (data points): These represent actual measurements or observations. The dispersion of these points around the surface indicates the model's accuracy—closely aligned points suggest a good fit, while widely spread points indicate potential deviations. This plot essentially helps to visualize and interpret the effect of robot geometry and pesticide volume on the plant scan time, guiding optimizations for efficient pesticide spraying.

Linear model Poly55:

f(x,y) = p00+p10*x + p01*y + p20*x^2 + p11*x*y + p02*y^2 + p30*x^3 + p21*x^2*y+p12*x*y^2+ p03*y^3 + p40*x^4 + p31*x^3*y +p22*x^2*y^2+ p13*x*y^3+p04*y^4+p50*x^5+p41*x^4*y+p32*x^3 *y^2+p23*x^2*y^3+ p14*x*y^4 + p05*y^5

Where x is normalized by mean 8.092 and standard 1.994 and where y is normalized by mean 0.01249 and standard 0.0002645

Coefficients (with 95% confidence bounds):

p00 =3.875e-05 (3.752e-05, 3.999e-05)

p10 = -1.66e-08 (-2.01e-06, 1.977e-06)

p01 = -1.709e-06 (-3.781e-06, 3.636e-07)

p20 = -3.391e-07 (-2.03e-06, 1.352e-06)

p11 = -1.327e-07 (-1.734e-06, 1.469e-06)

p02 = 5.065e-08 (-1.765e-06, 1.866e-06)

p30= -7.161e-08 (-1.528e-06, 1.385e-06)

p21= 3.078e-07 (-1.381e-06, 1.996e-06)

p12= -7.751e-08 (-2.304e-06, 2.149e-06)

p03 = 2.406e-06 (5.017e-09, 4.807e-06)

p40 = 3.322e-08 (-4.523e-07, 5.187e-07)

p31 = 2.183e-07 (-4.245e-07, 8.611e-07)

p22 =1.372e-07 (-8.643e-07, 1.139e-06)

p13 =1.074e-07 (-4.377e-07, 6.526e-07)

p04 = -2.865e-08 (-4.963e-07, 4.39e-07)

p50 = 2.586e-08 (-2.741e-07, 3.259e-07)

p41 = -6.924e-08 (-4.727e-07, 3.342e-07)

p32 = -2.801e-07 (-9.627e-07, 4.026e-07)

p23 = -1.697e-07 (-7.335e-07, 3.941e-07)

p14 = 2.254e-07 (-2.948e-07, 7.457e-07)

p05 = -5.232e-07 (-1.065e-06, 1.823e-08)

These model evaluation metrics suggest that the model may not be fitting the data well, despite the very low SSE and RMSE. Below is an interpretation of each metric in this context:

SSE (Sum of Squared Errors) – 5.327e-10: This extremely low SSE value suggests that the model's predictions are very close to the observed values on an absolute scale, with minimal error in terms of raw squared differences. However, SSE alone does not indicate how well the model captures the underlying pattern in the data.

Goodness of fit:

SSE	5.327e-10
R-square	0.108
Adjusted R-square	-0.07042
RMSE	2.308e-06

R-squared (0.108): An R-squared value of 0.108 means that only about 10.8% of the variance in the dependent variable (likely πd1 or πd2) is explained by the model. This low R-squared suggests that, while the predictions have low absolute error, the model does not capture much of the actual variability in the data. It may indicate that the model is over fitting or not effectively explaining the relationships in the data.

Adjusted R-squared (-0.07042): The negative Adjusted R-squared value suggests that the model may perform worse than a simple mean-based model. In other words, the added predictors (independent variables) do not contribute meaningful explanatory power and might even introduce noise into the model. This often indicates poor fit or over fitting, where the model captures noise rather than general patterns.

RMSE (Root Mean Square Error) – 2.308e-06: The RMSE is very low, consistent with the low SSE, meaning the average prediction error is extremely small. However, like SSE, a low RMSE does not necessarily mean that the model captures the underlying trends if the R-squared values are poor.

3.3 Development of response surface model for plant scan time

The relationship between several variables in the model as shown in Figure 3, similar to the previous one, but with πd2 on the vertical axis.

Below is a breakdown of what each element represents:

Vertical axis (πd2): This axis represents a new dependent variable related to the model. πd2 could correspond to another parameter tied to the spraying robot's performance or efficiency, potentially reflecting a different aspect of the robot's operational time or effectiveness in covering the plants.

Horizontal axes: π1π2: Represents the combined influence of robot geometry (π1) and another parameter, likely related to the robot or spraying configuration.π3π4: Represents the combined effect of pesticide volume parameters, including factors such as spray volume or nozzle flow rate.

Surface model representation: The surface model in the graph displays the estimated relationship between πd2 and the combined values of π1π2 and π3π4.

Surface shape: The presence of peaks and valleys suggests that πd2 has a non-linear dependency on these variables, with certain ranges of π1π2 and π3π4 leading to higher or lower values of πd2.

Data points: The black dots represent actual data values or observations, showing how the model's predictions (the surface) compare to real measurements.

A close alignment of the dots with the surface indicates a good model fit, while scattered points suggest areas where the model may not capture all the variability in the data.

Significance of the plot: This visualization helps in understanding the combined effects of robot geometry and pesticide volume on πd2, aiding in the identification of optimal configurations for improving the robot's performance.

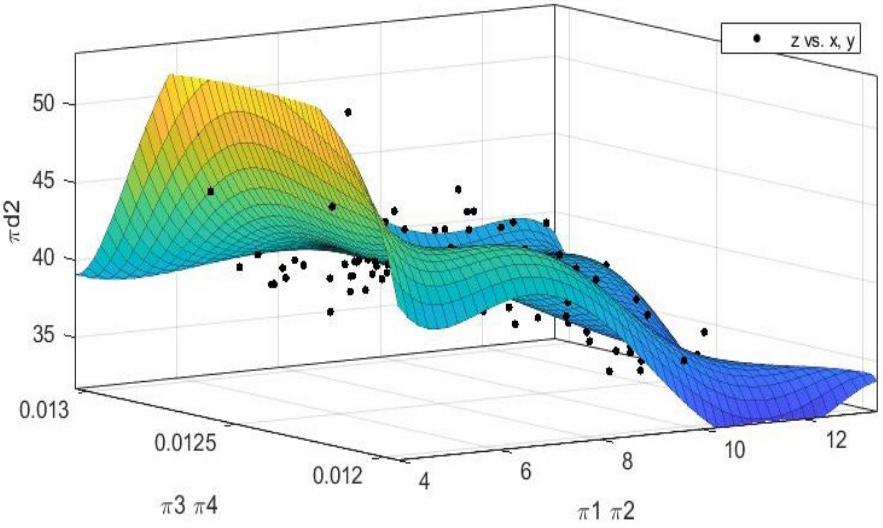

Figure 3 Graphical representation of response surface model for plant scan time

These statistics provide insights into the performance of the model shown in the 3D plot for predicting the dependent variable (πd2). Here's what each metric indicates SSE (Sum of Squared Errors) 539.7 SSE measures the total squared differences between the observed values and the values predicted by the model. A lower SSE indicates a better fit, as it means the predictions are closer to the actual observations. However, SSE alone doesn't provide context for how well the model performs relative to the overall variability in the data. R-square (0.6547) R-square, or the coefficient of determination, indicates the proportion of variance in the dependent variable (πd2) that is explained by the independent variables in the model. An R-square of 0.6547 means that around 65.47% of the variability in πd2 is explained by the model. This is a moderate level of explanation, suggesting that the model captures a significant portion of the data's variability but leaves some unexplained. Adjusted R-square (0.5856) Adjusted R-square adjusts the R-square value to account for the number of predictors in the model, providing a more accurate measure of goodness-of-fit when multiple variables are used. An Adjusted R-square of 0.5856 is slightly lower than the R-square, indicating that some variability might be due to noise or less relevant variables. This metric is useful for assessing if adding more variables significantly improves the model. RMSE (Root Mean Square Error) 2.323 RMSE measures the average magnitude of the residuals or prediction errors. It gives an idea of the model's prediction accuracy in the units of the dependent variable (πd2). An RMSE of 2.323 indicates that, on average, the model's predictions deviate from the actual values by about 2.323 units. Lower RMSE values imply better model accuracy. Figure 4 shows the close alignment between the two lines suggests the calculated model accurately predicts or describes the behaviour observed experimentally, with minor discrepancies likely due to experimental variability.

Linear model Poly55:

F (x, y) = p00 + p10*x + p01*y + p20*x^2 + p11*x*y + p02*y^2 + p30*x^3 + p21*x^2*y +p12*x*y^2 + p03*y^3 + p40*x^4 + p31*x^3*y + p22*x^2*y^2 + p13*x*y^3 + p04*y^4 + p50*x^5 + p41*x^4*y + p32*x^3*y^2 + p23*x^2*y^3 + p14*x*y^4 + p05*y^5

Where x is normalized by mean 8.092 and standard 1.994 and where y is normalized by mean 0.01249 and standard 0.0002645

Coefficients (with 95% confidence bounds):

p00 =39.97 (38.72, 41.21)

p10 =-2.525 (-4.531, -0.5185)

p01 =1.099 (-0.9868, 3.185)

p20 = -0.6337 (-2.336, 1.069)

p11 =0.9835 (-0.6283, 2.595)

p02 =0.7858 (-1.041, 2.613)

p30 =0.3124 (-1.153, 1.778)

p21 =0.5633 (-1.136, 2.263)

p12 =-0.1498 (-2.391, 2.091)

p03 =-1.819 (-4.236, 0.5976)

p40 =0.4912 (0.002506, 0.9798)

p31 =-0.0484 (-0.6954, 0.5986)

p22 =-0.5433 (-1.551, 0.4648)

p13 =-0.04823 (-0.597, 0.5005)

p04 =-0.1243 (-0.595, 0.3464)

p50 =-0.2271 (-0.5291, 0.07484)

p41 =-0.02778 (-0.4338, 0.3783)

p32 = 0.3488 (-0.3384, 1.036)

p23 =-0.1301 (-0.6975, 0.4374)

p14 =-0.0878 (-0.6115, 0.4359)

p05 =0.4377 (-0.1073, 0.9827)Goodness of fit:

SSE:	539.7
R-square:	0.6547
Adjusted R-square:	0.5856
RMSE:	2.323

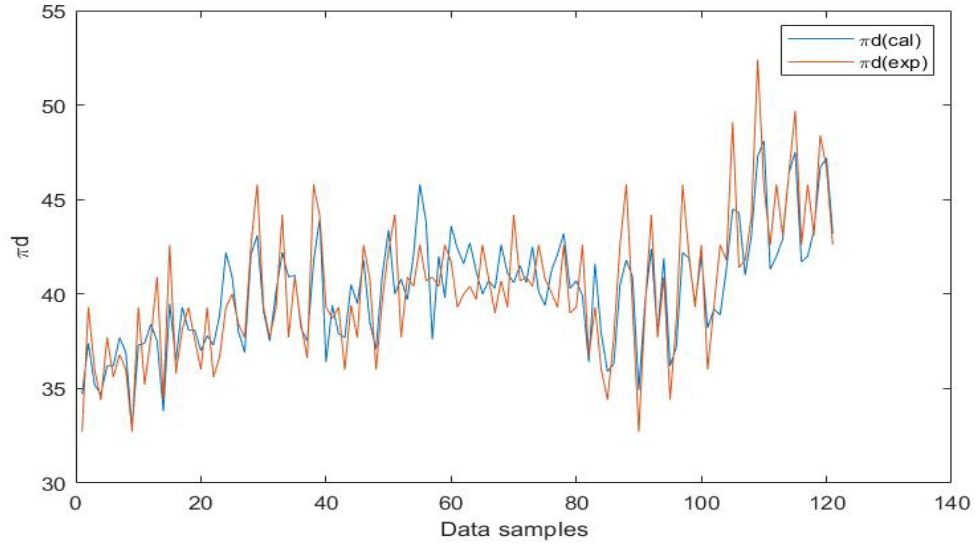

Figure 4 Calculated vs. experimental values for plant scan time

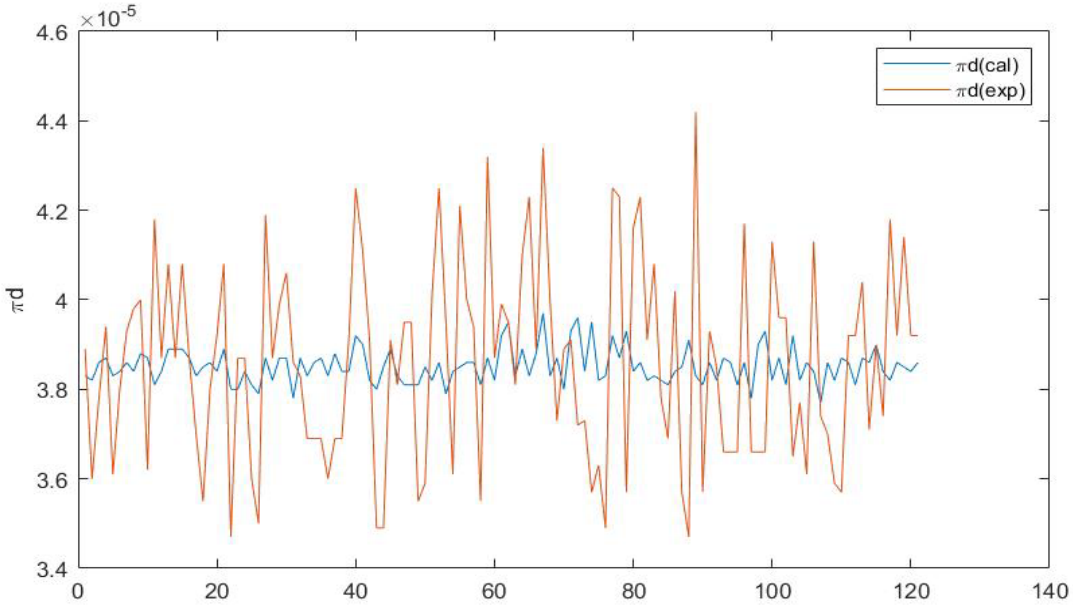

Figure 5 Experimental model and calculated model for pesticide quantity spread

Table 6 Sample calculation for percentage error between experimental, linear regression, and artificial neural network

Multiple Regression	%Error	Polynomial	%Error	RSM	% Error
1.4988		1.4988		5.6297	
5.8359		5.8359		14.8401	
2.1099		2.1099		8.8974	
1.8612		1.8612		2.6687	
5.5244		5.5244		18.3594	
1.1208		1.1208		6.0638	
1.8497		1.8497		3.2132	
3.5677		3.5677		1.9682	
2.9631		2.9631		0.9416	
6.4750		6.4750		11.7794	
8.8183		8.8183		3.1330	
0.6976		0.6976		6.7721	
4.7249		4.7249		0.5886	
0.6031		0.6031		4.1896	
4.4702		4.4702		1.7506	
0.0011		0.0011		4.0956	
3.4281		3.4281		8.3705	
7.9145		7.9145		13.4424	
1.6080		1.6080		5.8584	
1.9712		1.9712		3.1852	
4.8122		4.8122		1.1200	
8.8875		8.8875		14.4768	
1.7750		1.7750		4.4749	

The parameter related to the dynamics of a pesticide-spraying robot, the consistency of model in predicting robot behavior under controlled conditions. Where experimental factors (e.g., actuator noise, environmental effects) introduce deviations, which might need to be addressed for better control and stability as shown in Figure 5. 3.4 Evaluation and interpretation of experimental errors

The error is the difference between a calculated value and an experimental value. If the error is less than the condition of the experiment or measurement is said to be accurate which helps to create good and accurate mathematical correlations between output and input below table shows the sample calculation between experimental, linear regression, and Artificial neural network as shown in table 6.

The percentage error for three different modelling techniques. Each row in the table represents a different experimental or test case, showing how each model performed in terms of prediction accuracy. The percentage error quantifies the deviation of the predicted values from the actual values, with lower values indicating better accuracy. Multiple Regression and ppolynomial regression produce identical error values for each case, suggesting that the polynomial model used might be similar to or derived from the multiple regression model. RSM tends to have higher errors compared to the other two methods in many cases, particularly in cases like row 2 (14.8401%) and row 5 (18.3594%). This suggests that RSM may not be the most precise approach for this dataset. In some cases, RSM outperforms the other models (e.g., row 13 with 0.5886% error), indicating that it may work well under specific conditions. The error values fluctuate across different cases, indicating variability in model performance depending on the dataset characteristics.

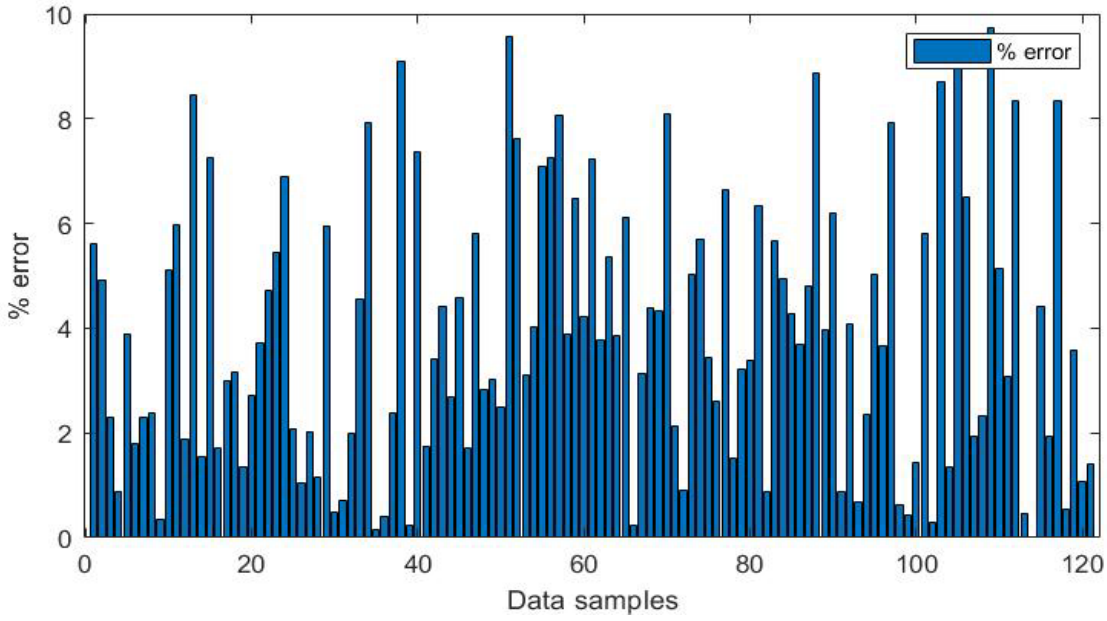

Figure 6 Error analysis of plant scan time using MRA Model

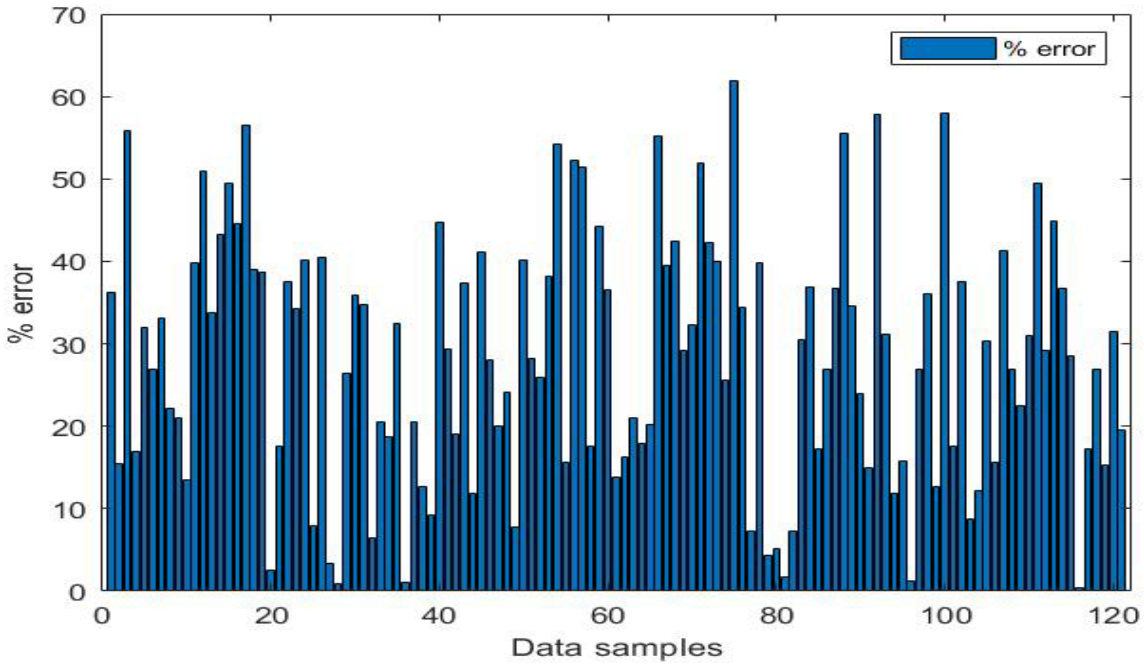

Figure 7 Error prediction in pest detection using MRA Model

The calculated line represents the expected behaviour of a theoretical model as shows in Figure 6. Its smoothness suggests a well-behaved and deterministic prediction. The experimental line has much greater variability, but its overall mean trend is similar to the calculated line, indicating that the model captures the general behaviour of the system.

The model is effective in predicting trends. Experimental noise or disturbances need to be mitigated to achieve closer alignment between calculated and observed results as shows in Figure 7. Additional analysis of the discrepancies can help improve the robot's reliability and precision in real-world agricultural applications. The dimensionless π-groups, which are formed using dimensional analysis represents in table 7 (typically with the Buckingham Pi theorem) to describe the relationships between different variables in your system.

Three columns of numerical data for 20 different test cases or conditions. However, without specific variable names, it provide a general interpretation based on the pattern and typical uses of such datasets

shown in Table 8.

Table 7 Identification and analysis of independent parameters

Sr. No.	π1 $\left[\frac{BH_rMN}{DL_1\omega F}\right]$	π2 $\left[\frac{H_pL}{H^2}\right]$	π3 $[\alpha]$	π4 $\frac{Vt}{H^3}$
1	1.73E+01	7.31E-01	9.50E-01	1.31E-02
2	1.48E+01	7.78E-01	9.70E-01	1.31E-02
3	1.62E+01	7.15E-01	9.60E-01	1.31E-02
4	1.57E+01	6.86E-01	9.40E-01	1.31E-02
5	1.67E+01	7.76E-01	9.80E-01	1.31E-02
6	1.40E+01	7.14E-01	9.30E-01	1.31E-02
7	1.30E+01	7.27E-01	9.60E-01	1.31E-02
8	1.40E+01	7.34E-01	9.50E-01	1.31E-02
9	1.72E+01	6.47E-01	9.20E-01	1.31E-02
10	1.35E+01	7.20E-01	9.70E-01	1.31E-02
11	1.36E+01	7.58E-01	9.40E-01	1.31E-02
12	1.34E+01	7.66E-01	9.80E-01	1.31E-02
13	1.27E+01	7.01E-01	9.60E-01	1.31E-02
14	1.58E+01	6.49E-01	9.30E-01	1.31E-02
15	1.15E+01	7.29E-01	9.90E-01	1.31E-02
16	1.25E+01	6.73E-01	9.20E-01	1.31E-02
17	1.16E+01	7.55E-01	9.50E-01	1.31E-02
18	1.31E+01	7.45E-01	9.70E-01	1.31E-02
19	1.18E+01	7.07E-01	9.40E-01	1.31E-02
20	1.35E+01	7.27E-01	9.40E-01	1.31E-02

Table 8 Sample calculation for dependent variable

Sr. No.	$\pi_{d1} = \left[\frac{Vs}{H^3}\right]$	$\pi_{d2} = \left[\sqrt{\frac{g}{H}}t\right]$	π_{d3} = [n]
1	3.27E+01	3.89E-05	6
2	3.93E+01	3.60E-05	9
3	3.60E+01	3.78E-05	9
4	3.44E+01	3.94E-05	6
5	3.77E+01	3.61E-05	7
6	3.56E+01	3.80E-05	6
7	3.68E+01	3.93E-05	6
8	3.60E+01	3.98E-05	7
9	3.27E+01	4.00E-05	9
10	3.93E+01	3.62E-05	7
11	3.52E+01	4.18E-05	6
12	3.77E+01	3.87E-05	7
13	4.09E+01	4.08E-05	9
14	3.44E+01	3.87E-05	7
15	4.26E+01	4.08E-05	6
16	3.58E+01	3.87E-05	8
17	3.81E+01	3.70E-05	7
18	3.93E+01	3.55E-05	8
19	3.76E+01	3.80E-05	7
20	3.60E+01	3.92E-05	6

3.5 Influence of model indices on experimental outcomes

The indices of models are the indicator of the behavior of the phenomenon, it indicate how the phenomenon is affected because of the interaction of various independent π terms in the model. The constants and indices of independent π term are given in the Table 9.

3.6 Model Analysis for the Dependent π Term in Pesticide Application (πd1)

The model for the dependent π term πd1 is as under

$$\pi d1 = \left[\frac{Vs}{H^3}\right] = 725.604 \times \left[\frac{BH_rMN}{DL_1\omega F}\right]^{-0.0119} \times \left[\frac{H_pL}{H^2}\right]^{-0.1686} \times [\alpha]^{0.2468} \times \left[\frac{Vt}{H^3}\right]^{3.8664} \quad (15)$$

The following primary conclusion appears to be justified from the above model.

The absolute index value of π1 is -0.0119 is related

to the geometry of robot is the least influencing term in this model. The value of this index term is negative. The negative index shows that $\pi 1$ is inversely proportional to $\pi d1$.

The absolute index value of $\pi 2$ is -0.1686. The term $\pi 2$ is related to the plant is moderately influencing term in this model. The value of this index term is negative. The negative index indicate $\pi 2$ is inversely proportional to $\pi d1$.

The absolute index value of $\pi 3$ is second largest viz. 0.2468. The term $\pi 3$ is related to the sensor which significantly influencing the dependent variable $\pi d1$ term in this model. The positive index indicates that $\pi 3$ is directly proportional to $\pi d1$.

The absolute index value of $\pi 4$ is highest viz. 3.8664. The term $\pi 4$ is related to the pesticide volume is the most influencing term in this model. The positive index indicating that $\pi 4$ is directly proportional $\pi d1$.

3.7 Model Evaluation for the Dependent Pi Term in Plant Scan Time

The model for the dependent pi term $\pi d2$ is as under:

$$\pi d2 = \left[\sqrt{\frac{g}{H}}t\right] = 1.691 \times \left[\frac{BH_rMN}{DL_1\omega F}\right]^{-0.2841} \times \left[\frac{H_pL}{H^2}\right]^{0.362} \times [\alpha]^{0.3698} \times \left[\frac{Vt}{H^3}\right]^{-0.9143} \quad (16)$$

The absolute index value of $\pi 1$ is lowest viz. -0.2841. The term $\pi 1$ is related to the geometry of robot is the least influencing term in this model. The value of this index term is negative. The negative index indicates that $\pi 1$ is inversely proportional to $\pi d2$.

The absolute index value of $\pi 2$ is third largest viz. 0.362. The term $\pi 2$ is related to the plant is the significantly influencing term in this model. The value of this index term is positive indicating $\pi 2$ is directly proportional to$\pi d2$.

The absolute index value of $\pi 3$ is second largest viz. 0.3698. The term $\pi 3$ is related to the sensor is the second most influencing term in this model. The value of this index term is positive indicating $\pi 3$ is directly proportional to $\pi d2$.

The absolute index value of $\pi 4$ is -0.9143 is related to the pesticide quantity spread is the most influencing term in this model. The value of this index term is negative. The negative index $\pi 4$ varies inversely with respect to $\pi d2$.

Table 9 Constants and indices for response variables in robotic systems

π term	$\pi d1$	$\pi d2$	$\pi d3$
K	725.604	1.69199	0.84800
$\pi 1$	-0.0119	-0.2841	-0.0081
$\pi 2$	-0.1686	0.362	0.2966
$\pi 3$	0.2468	0.3698	-0.0259
$\pi 4$	3.8664	-0.9143	-0.5265

4 Discussion

The research demonstrates that the application of robotic pesticide spraying enhances precision, reduces human exposure, and optimizes pesticide usage. The proposed mathematical model successfully integrates the Buckingham Pi theorem for dimensional analysis, allowing for a more generalized approach to modelling motion controll in agricultural robotics. The results validate the feasibility of using autonomous robotic sprayers to achieve efficient pesticide distribution while maintaining sustainability.

The literature highlights significant advancements in agricultural automation, particularly in pesticide spraying robots. The integration of robotics, Artificial Intelligence, and control systems has improved the efficiency and precision of pesticide application while reducing human exposure to harmful chemicals. The Buckingham Pi theorem and dimensional analysis have proven valuable in simplifying complex interactions and enhancing model generalization, particularly in machine learning and motion control applications.

However, challenges remain, particularly regarding the applicability of dimensional analysis across different robotic systems and real-world agricultural settings. Most studies rely on simulated environments, necessitating further validation through field experiments. Future research should focus on refining mathematical models to accommodate varying agricultural conditions, improving the adaptability of dimensionless methods for diverse robotic applications, and integrating machine learning techniques to enhance pest prediction accuracy. Addressing these gaps will ensure more robust, efficient, and practical automated pesticide spraying solutions for sustainable agriculture. It leads to substantial savings in pesticide usage by ensuring precise and targeted application, thereby reducing chemical wastage and input costs. Second, automation minimizes the need for farm workers, which lowers operational expenses and addresses problem of workers shortages in the agricultural sector. Third, by optimizing spray uniformity and accuracy, robotic systems help improve plant health and yield, resulting in higher productivity and profitability for farmers. Additionally, intelligent control systems reduce over-spraying and environmental contamination, leading to lower long-term costs associated with soil and water remediation. The enhanced efficiency and data-driven operation also support predictive maintenance and better resource management, further reducing downtime and maintenance costs. Overall, the adoption of intelligent robotic spraying systems contributes to cost efficiency, higher yield quality, and sustainable agricultural practices, making them a highly economically viable solution for modern farming

5 Conclusion

This study underscores the critical hazards posed by the extensive use of pesticides in agriculture, particularly for individuals directly involved in field operations, such as farmers and farmworkers. To mitigate these risks, a dimensionless model derived through the Buckingham Pi theorem is proposed to optimize pesticide spraying techniques. This methodology is especially beneficial in the context of robotic systems used for cotton crop cultivation, as it integrates essential parameters including pesticide dosage and plant scan time. The proposed model, formulated using real-time data, facilitates a robust framework for enhancing the efficiency, accuracy, and safety of pesticide application. By establishing predictive relationships between influential variables both dependent and independent the model enables comprehensive analysis of factors governing the spraying process. This predictive capability is instrumental in minimizing human exposure to harmful chemicals, thereby promoting a healthier agricultural environment. Furthermore, the integration of this model into mobile robotic platforms supports the development of intelligent, adaptive spraying systems. Such systems not only optimize pesticide usage but also contribute to the creation of a safer and more efficient working environment. The adoption of this innovative approach is essential for advancing precision agriculture and safeguarding the well-being of agricultural labourers.

Conflicts of interest

The authors have no conflicts of interest to declare.

Data Availability

The data supporting this study findings are confidential and cannot be shared publically due to legal and privacy restrictions. As a result, data are not available for external use.

References

Abade, A., P. A. Ferreira, and F. de Barros Vidal. 2021. Plant diseases recognition on images using convolutional neural networks: A systematic review. *Computers and Electronics in Agriculture*, 185: 106125.

Bakarji, J., J. Callaham, S. L. Brunton, and J. N. Kutz. 2022. Dimensionally consistent learning with Buckingham Pi. *Nature Computational Science*, 2(12): 834–844.

Bechar, A., and C. Vigneault. 2016. Agricultural robots for field operations: Concepts and components. *Biosystems Engineering*, 149: 94-111.

Bhute, N. K., C. S. Patil, K. V. Deshmukh, R. S. Wagh, and N.

K. Medhe. 2023. Pink bollworm Pectinophora gossypiella (Saunders), a destructive pest of cotton: a review. *The Pharma Innovation Journal*, 12(3): 2036–2042.

Bucelli, M., A. Zingaro, P. C. Africa, I. Fumagalli, L. Dede', and A. Quarteroni. 2023. A mathematical model that integrates cardiac electrophysiology, mechanics, and fluid dynamics: Application to the human left heart. *International Journal for Numerical Methods in Biomedical Engineering*, 39(3): 3678.

Budiharto, W., A. Chowanda, A. A. S. Gunawan, E. Irwansyah, and J. S. Suroso. 2019. A Review and Progress of Research on Autonomous Drone in Agriculture, Delivering Items and Geographical Information Systems (GIS). In *Proc. 2019 2nd World Symposium on Communication Engineering*, 205–209. Nagoya, Japan, 20-23 December.

Čarnogurská, M., M. Příhoda, M. Andrejiová, and L. Tóth. 2024. Analysis of the Mathematical Models for Identifying the Thickness of the Fouling Layer in Natural Gas Coolers. *Applied Sciences*, 14(10): 4003.

Chouriya, A., P. Soni, S. Hota, and E. V. Thomas. 2024. Ergonomic Evaluation of a Walk-Behind AI-Based Cotton Fertilizer Applicator. *Journal of Field Robotics*, 42(5): 1826-1839.

Dhutekar, P., G. Mehta, J. Modak, S. Shelare, and P. Belkhode. 2021. Establishment of mathematical model for minimization of human energy in a plastic moulding operation. *Materials Today: Proceedings*, 47(14): 4502–4507.

Dou, H., Q. Li, C. Zhai, S. Yang, C. Zhao, Y. Gao, and Y. He. 2023. Computational model of pesticide deposition distribution on canopies for air-assisted spraying. *Frontiers in Plant Science*, 14: 1153904.

Dubey, H. K., M. P. Singh, M. Giripunje, and R. Kawalkar. 2022. Formulation of mathematical model using dimensional analysis approach for plastic shredding process through Human powered flywheel Motor (HPFM). *Materials Today: Proceedings*, 50: 1700–1707.

Fue, K. G., W. M. Porter, E. M. Barnes, and G. C. Rains. 2020. An Extensive Review of Mobile Agricultural Robotics for Field Operations: Focus on Cotton Harvesting. *AgriEngineering*, 2(1): 150–174.

Fukami, K., S. Goto, and K. Taira. 2024. Data-driven nonlinear turbulent flow scaling with Buckingham Pi variables. *Journal of Fluid Mechanics*. 984

García-Alegre, M. C., A. Ribeiro, L. García-Pérez, R. Martínez, D. Guinea, and A. Pozo-Ruz. 2001. Autonomous robot in agriculture tasks. In *3th European Conference on Precision Agriculture*, 25–30.

Girard, A. 2024. Dimensionless Policies Based on the Buckingham π Theorem. *Mathematics*, 12(5): 709.

Gu, Y., L. Bouvier, A. Tonda, and G. Delaplace. 2019. A mathematical model for the prediction of the whey protein fouling mass in a pilot scale plate heat exchanger. *Food Control*, 106: 106729.

Han, C., J. Lv, C. Dong, J. Li, Y. Luo, W. Wu, and M. A. Abdeen. 2024. Classification, advanced technologies, and typical applications of end-effector for fruit and vegetable picking robots. *Agriculture*, 14(8): 1310.

Ilyushin, Y. V., and E. I. Kapostey. 2023. Developing a Comprehensive Mathematical Model for Aluminium Production in a Soderberg Electrolyser. *Energies*, 16(17): 6313.

Jat, D., K. Dubey, R. R. Potdar, S. K. Chakraborty, S. P. Kumar, N. S. Chandel, Y. A. Rajwade, and A. Subeesh. 2023. Development of an automated mobile robotic sprayer to prevent workers' exposure of agro-chemicals inside polyhouse. *Journal of Field Robotics*, 40(6): 1388–1407.

Kassim, A. M., M. Termezai, A. Jaya, A. H. Azahar, S. Sivarao, F. A. Jafar, H. I. Jaafar, M. S. M. Aras. 2020. Design and development of autonomous pesticide sprayer robot for fertigation farm. *International Journal of Advanced Computer Science and Applications*, 11(2): 545–551.

Kaushik, V., and R. N. Shankar. 2021. Review of Experimental Approaches for the Analysis of Aerodynamic Performance of Vertical Axis Wind Turbines. In *Innovative Design, Analysis and Development Practices in Aerospace and Automotive Engineering*, eds. N. Gascoin, and E. Balasubramanian, 473–480.

Kaushik, V., and N. Shankar. 2022. Statistical Analysis using Taguchi Method for Designing a Robust Wind Turbine. *Journal of Advanced Research in Fluid Mechanics and Thermal Sciences*, 100(3): 92–105.

Kaushik, V., R. N. Shankar, N. I. H. Rashid, and P. B. Khope. 2022. Implementation of Taguchi method for designing a robust wind turbine. *Transdisciplinary Journal of Engineering & Science*, SP-2: 165-185.

Li, C., J. Wu, X. Pan, H. Dou, X. Zhao, Y. Gao, S. Yang, and C. Zhai. 2023. Design and experiment of a breakpoint continuous spraying system for automatic-guidance boom sprayers. *Agriculture*, 13(12): 2203.

Lochan, K., A. Khan, I. Elsayed, B. Suthar, L. Seneviratne, and I. Hussain. 2024. Advancements in Precision Spraying of Agricultural Robots: A Comprehensive Review. *IEEE Access*, 12: 129447 - 129483.

Luo, X., F. Xie, X. Liu, and Z. Xie. 2021. Kinematic calibration of a 5-axis parallel machining robot based on dimensionless error mapping matrix. *Robotics and Computer-Integrated Manufacturing*, 70:102115.

Lv, H., L. Kang, and Y. Liu. 2024. Dimensional analysis and effects of dimensionless numbers on the iron removal process in electromagnetic induction heating furnaces.

International Journal of Heat and Mass Transfer, 229: 125714.

Meshram, A., A. Vanalkar, K. Meshram, A. Badar, G. Mehta, and V. Kaushik. 2024. Enhancing crop protection through smart autonomous pesticide spray bot in sustainable agriculture. *Engineering Research Express*, 6(4): 045563.

Meshram, A., A. Vanalkar, K. Kalambe, A. Badar, V. Kaushik, and G. Mehta. 2024. Experimental investigation on natural fiber material for pesticide spraying mobile robot structure. *Materials Today: Proceedings*,

Normey-Rico, J. E., I. Alcalá, J. Gómez-Ortega, and E. F. Camacho. 2001. Mobile robot path tracking using a robust PID controller. *Control Engineering Practice*, 9(11): 1209–1214.

Olabi, A. G., H. M. Maghrabie, O. H. K. Adhari, E. T. Sayed, B. A. A. Yousef, T. Salameh, M. Kamil, and M. A. Abdelkareem. 2022. Battery thermal management systems: Recent progress and challenges. *International Journal of Thermo fluids*, 15: 100171.

Ozgul, E., and U. Celik. 2018. Design and implementation of semi-autonomous anti-pesticide spraying and insect repellent mobile robot for agricultural applications. In *2018 5th International Conf. on Electrical and Electronic Engineering*, 233–237.

Pandey, S. K., P. K. Ojha, and K. Roy. 2020. Exploring QSAR models for assessment of acute fish toxicity of environmental transformation products of pesticides (ETPPs). *Chemosphere*, 252: 126508.

Prakash, C., S. Singh, A. Pramanik, A. Basak, G. Królczyk, M. Bogdan-Chudy, Y. Wu, H. Y. Zheng. 2021. Experimental investigation into nano-finishing of β-TNTZ alloy using magnetorheological fluid magnetic abrasive finishing process for orthopedic applications. *Journal of Materials Research and Technology*, 11: 600–617.

Prechsl, U. E., M. Bonadio, L. Wegher, and M. Oberhuber. 2022. Long-term monitoring of pesticide residues on public sites : A regional approach to survey and reduce spray drift. *Frontiers in Environmental Science*, 10: 1062333.

Ramesh, A. P., and N. Pasupathy. 2019. Design and implementation of remote sensing robotic platform for precision agriculture. *International Journal of Innovation Technology Exploration. Engineering.* 8(11): 2396–2399.

Ray, S., M. Haque, T. Ahmed, and T. T. Nahin. 2023. Comparison of artificial neural network (ANN) and response surface methodology (RSM) in predicting the compressive and splitting tensile strength of concrete prepared with glass waste and tin (Sn) can fiber. *Journal of King Saud University – Engineering Sciences*, 35(3): 185–199.

Reji, M., and R. Kumar. 2022. Response surface methodology (RSM): An overview to analyze multivariate data. *Indian Journal of Microbiological Research*, 9(4): 241-248.

Salotti, J. M., and E. Suhir. 2024. Collaborative Robotics: Application of Delphi Method. *Journal of Field Robotics*, 42(5): 1799-1807.

Shaw, K. K., and R. Vimalkumar. 2020. Design and Development of a Drone for Spraying Pesticides, Fertilizers and Disinfectants. *International Journal of Engineering Research & Technology*, 9(05): 1181–1185.

Song, Y., H. Sun, M. Li, and Q. Zhang. 2015. Technology Application of Smart Spray in Agriculture: A Review. *Intelligent Automation & Soft Computing*, 21(3): 319–333.

Sritham, E., N. Nunak, E. Ongwongsakul, J. Chaishome, G. Schleining, and T. Suesut. 2023. Development of Mathematical Model to Predict Soymilk Fouling Deposit Mass on Heat Transfer Surfaces Using Dimensional Analysis. *Computation*, 11(4): 83.

Sulaiman, M., M. Umar, K. Nonlaopon, and F. S. Alshammari. 2022. The Quantitative Features Analysis of the Nonlinear Model of Crop Production by Hybrid Soft Computing Paradigm. *Agronomy*, 12(4): 799.

Trivedi, N. K., V. Gautam, A. Anand, H. M. Aljahdali, S. G. Villar, D. Anand, N. Goyal, and S. Kadry. 2021. Early detection and classification of tomato leaf disease using high-performance deep neural network. *Sensors*, 21(23): 7987.

Villar, S., W. Yao, D. W. Hogg, B. Blum-Smith, and B. Dumitrascu. 2022. Dimensionless machine learning: Imposing exact units equivariance. *Journal of Machine Learning Research*, 24(109): 1-32.

Xie, X., A. Samaei, J. Guo, W. K. Liu, and Z. Gan. 2022. Data-driven discovery of dimensionless numbers and governing laws from scarce measurements. *Nature Communications*, 13(1): 7562.

Zhang, K., K. Lammers, P. Chu, Z. Li, and R. Lu. 2024. An automated apple harvesting robot from system design to field evaluation. *Journal of Field Robotics*, 41(7): 2384–2400.